Proceedings of IMECE'01
2001 ASME International Mechanical Engineering Congress and Exposition
November 11-16, 2001, New York, New York, USA

IMECE01/DSC-4A-3

NONLINEAR MODEL BASED COORDINATED ADAPTIVE ROBUST CONTROL OF ELECTRO-HYDRAULIC ROBOTIC MANIPULATORS: METHODS AND COMPARATIVE STUDIES *

Fanping Bu and Bin Yao +
School of Mechanical Engineering
Purdue University
West Lafayette, IN 47907
+ Email: byao@ecn.purdue.edu

ABSTRACT

Compared to conventional robot manipulators driven by electrical motors, hydraulic robot arms have richer nonlinear dynamics and stronger couplings among various joints (or hydraulic cylinders). This paper focuses on the physical model based coordinated adaptive robust control (ARC) strategies that explicitly take into account the strong coupling among various hydraulic cylinders (or joints). In our recent studies, two such methods were proposed to avoid the need of acceleration feedback in doing ARC backstepping designs. The first method uses an observer to recover the state needed for the ARC backstepping design. The second method utilizes the property that the adjoint matrix and the determinant of the inertial matrix can be linearly parametrized by certain suitably selected parameters and employ certain over-parametrizing techniques. Theoretically, both the resulting ARC controllers guarantee a prescribed output tracking transient performance and final tracking accuracy while achieving asymptotic output tracking in the presence of parametric uncertainties only. This paper focuses on the comparative studies of these two methods under various practical constraints. Extensive simulation results which are based on a three degree-of-freedom (DOF) hydraulic robot arm are presented to illustrate the advantages and drawbacks of each method.

1 Introduction

Robotic manipulators driven by electro-hydraulic cylinders have been widely used in the industry for the tasks such as material handling and earth moving. These kinds of tasks typically require that the end-effectors of the manipulators follow certain prescribed desired trajectories in the working space precisely. In order to meet the increasing requirement of productivity and performance of modern industry, the development of high speed and high accuracy trajectory tracking controllers for robot manipulators is of practical importance.

Compared to the the conventional robotic manipulator driven by electrical motors, the controller design for the robotic manipulator driven by hydraulic actuators is more difficult both theoretically and experimentally due to the following several reasons. First of all, unlike the electrical motors, the hydraulic cylinders are linear actuators and complicated mechanical mechanisms are needed to drive revolute joints. Such a configuration results in additional nonlinearites and stronger couplings among the dynamics of various joints. Second, in addition to the coupled MIMO nonlinear dynamics of the rigid robot arm, the dynamics of the hydraulic actuators must be considered in the control of a hydraulic arm, which substantially increases the controller design difficulties. It is well known that a robot arm including actuator dynamics (Yuan, 1995) has a "relative degree" more than three. Synthesizing a controller for such a system usually requires joint acceleration feedback for a complete state feedback, which may not be a practical solution. Furthermore, the single-rod hydraulic actuator studied here has a much more complicated dynamics than electrical motors. The dynamics of a hydraulic cylinder is highly nonlinear (Merritt, 1967) and may be subjected to non-smooth and discontinuous nonlinearities due to directional change of valve opening and frictions. The dynamic equations describing the pressure changes in the two chambers of a single-rod hydraulic actuator cannot be combined into a single load pressure equation, which not only increases the dimension

* THE WORK IS SUPPORTED IN PART BY THE NATIONAL SCIENCE FOUNDATION UNDER THE CAREER GRANT CMS-9734345 AND IN PART BY A GRANT FROM THE PURDUE ELECTRO-HYDRAULIC RESEARCH CENTER.

of the system to be dealt with but also brings in the stability issue of the added internal dynamics. Finally, a hydraulic arm normally experiences large extent of model uncertainties including the large changes in load seen by the system in industrial use, the large variations in the hydraulic parameters (e.g., bulk modulus), leakages, the external disturbances, and frictions. Partly due to these difficulties, so far, the model-based robust control of a hydraulic arm has not been well studied and fewer results are available. In (d'ANdrea Novel et al., 1994), the singular perturbation was used to synthesize a controller for a 6 axis hydraulically actuated robot. In (Medanic et al., 1997), a variable structure controller was developed to control a Caterpillar 325 excavator without considering parametric uncertainties and uncertain nonlinearities associated with the system simultaneously. Theoretically, none of above schemes could address all the difficulties mentioned above well.

In (Yao et al., 2000; Bu and Yao, 1999), the ARC approach proposed by Yao and Tomizuka in (Yao and Tomizuka, 1994; Yao and Tomizuka, 1997; Yao and Tomizuka, 2001; Yao, 1997) was generalized to provide a rigorous theoretical framework for the high performance robust motion control of a one DOF single-rod hydraulic actuator by taking into account the particular nonlinearities and model uncertainties of the electro-hydraulic servo-systems. The stability of zero output tracking error dynamics of single-rod hydraulic actuator was also addressed in (Yao et al., 2000; Bu and Yao, 1999). In (Bu and Yao, 2000), a physical model based ARC controller, which explicitly takes into account the strong coupling among various hydraulic cylinders (or joints), is proposed for a 3 DOF hydraulic robot arm. An observer which is motivated by the design in (Yuan, 1995) is proposed to avoid the need of acceleration feedback for ARC backstepping design. In (Bu and Yao, 2001), an overparametrizing method, which is motivated by the design in (Bridges et al., 1993), is proposed to avoid the need of acceleration feedback for ARC backstepping design.

This paper will continue the work done in (Bu and Yao, 2000; Bu and Yao, 2001) and will focus on the comparative studies of these two method under various practical implementation constraints such as the measurement noises. Extensive comparative simulation results will be presented to illustrate the advantages and drawbacks of each method.

2 Problem Formulation and Dynamic Models

The system under consideration is depicted in Fig.1, which represents a 3 DOF robot arm driven by three single-rod hydraulic cylinders. To make the results general, let us consider a n DOF robot arm driven by n hydraulic cylinders. The joint angles are represented by $q = [q_1, q_2, \ldots, q_n]^T$. $x = [x_1, x_2, \ldots, x_n]^T$ is the displacement vector of the hydraulic cylinders, which is uniquely related to the joint angle q, i.e., $x_1(q_1)$, $x_2(q_2)$ and so on. The goal is to have joint angles q track any feasible desired motion trajectories as closely as possible for precision maneuver of the inertia load of the hydraulic robot arm. The rigid-body

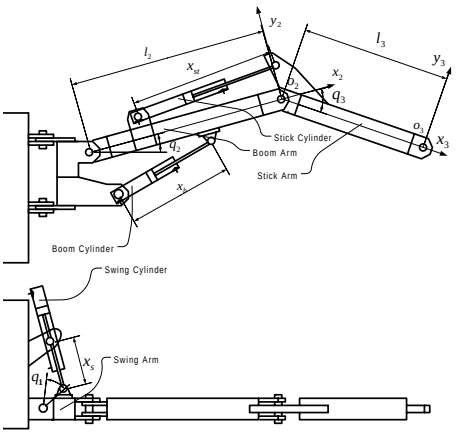

Figure 1. A Hydraulic Robot Arm

dynamics of the hydraulic arm can be described by:

$$M(q)\ddot{q} + C(q,\dot{q})\dot{q} + G(q) = \frac{\partial x}{\partial q}(A_1P_1 - A_2P_2) + T(t,q,\dot{q}) \quad (1)$$

where $P_1 = [P_{11}, P_{12}, \cdots, P_{1n}]^T$ and P_{1i} $(i = 1,2,\cdots,n)$ is the forward chamber pressures for the ith cylinder. $P_2 = [P_{21}, P_{22}, \cdots, P_{2n}]^T$ and P_{2i} $(i = 1,2,\cdots,n)$ is the return chamber pressure of the ith cylinder. $A_1 = diag[A_{11}, A_{12}, \cdots, A_{1n}]$ and $A_2 = diag[A_{21}, A_{22}, \cdots, A_{2n}]$ are the ram areas of the two chambers of the driving cylinders and $T(t,q,\dot{q}) \in R^n$ represents the lumped disturbance torque including external disturbances and terms like the friction torque.

Let m_L be the unknown payload mounted at the end of the nth arm, which is treated as a point mass for simplicity. Then, the inertial matrix $M(q)$, coriolis terms $C(q,\dot{q})$ and gravity terms $G(q)$ in (1) can be linearly parametrized with respect to the unknown mass m_L as

$$\begin{aligned} M(q) &= M_c(q) + M_L(q)m_L, G(q) = G_c(q) + G_L(q)m_L \\ C(q,\dot{q}) &= C_c(q,\dot{q}) + C_L(q,\dot{q})m_L \end{aligned} \quad (2)$$

where $M_c(q)$, $M_L(q)$, $C_c(q,\dot{q})$, $C_L(q,\dot{q})$, $G_c(q)$, $G_L(q)$ are known nonlinear functions of q and $\dot{q}$. One of the properties of the inertia matrix $M(q)$ is that its inverse can be written as:

$$M^{-1}(q) = \bar{M}(q)/|M(q)| \quad (3)$$

where $|M(q)|$ represents the determinant of $M(q)$, $\bar{M}(q)$ represents the adjoint matrix of $M(q)$. Furthermore, both $\bar{M}(q)$ and $|M(q)|$ can be written as

$$|M(q)| = I = I_c + \sum_{i=1}^{n} I_{si}m_L^i \quad \bar{M}(q) = \bar{M}_c + \sum_{i=1}^{n-1} \bar{M}_i m_L^i \quad (4)$$

where I_c, I_{si}, $\bar{M}_c$ and $\bar{M}_i$ are of the known functions of joint position q and I is a scalar.

Assuming no cylinder leakages, the actuator (or the cylinder) dynamics can be written as (Merritt, 1967),

$$\begin{array}{l} \frac{V_1(x)}{\beta_e}\dot{P}_1 = -A_1\dot{x} + Q_1 = -A_1\frac{\partial x}{\partial q}\dot{q} + Q_1 \\ \frac{V_2(x)}{\beta_e}\dot{P}_2 = A_2\dot{x} - Q_2 = A_2\frac{\partial x}{\partial q}\dot{q} - Q_2 \end{array} \quad (5)$$

where $V_1(x) = V_{h1} + A_1 diag[x] \in R^{n\times n}$ and $V_2(x) = V_{h2} - A_2 diag[x]$ are the diagonal total control volume matrices of the two chambers of hydraulic cylinders respectively, which include the hose volume between the two chambers and the valves, $V_{h1} = diag[V_{h11}, V_{h12}, \cdots, V_{h1n}]$ and $V_{h2} = diag[V_{h21}, V_{h22}, \cdots, V_{h2n}]$ are the control volumes of the two chambers when $x = 0$, $diag[x] = diag[x_1, x_2, \cdots, x_n]$, $\beta_e \in R$ is the effective bulk modulus, $Q_1 = [Q_{11}, Q_{12}, \cdots, Q_{1n}]^T$ is the vector of the supplied flow rates to the forward chambers of the driving cylinders, and $Q_2 = [Q_{21}, Q_{22}, \cdots, Q_{2n}]^T$ is the vector of the return flow rates from the return chambers of the cylinders.

Let $x_v = [x_{v1}, x_{v2}, \cdots, x_{vn}]$ denotes the spool displacements of the valves in the hydraulic loops. Define the square roots of the pressure drops across the two ports of the first control valve as:

$$\begin{array}{l} g_{31}(P_{11}, sign(x_{v1})) = \left\{ \begin{array}{ll} \sqrt{P_s - P_{11}} & \text{for } x_{v1} \geq 0 \\ \sqrt{P_{11} - P_r} & x_{v1} < 0 \end{array} \right. \\ g_{41}(P_{21}, sign(x_{v1})) = \left\{ \begin{array}{ll} \sqrt{P_{21} - P_r} & \text{for } x_{v1} \geq 0 \\ \sqrt{P_s - P_{21}} & x_{v1} < 0 \end{array} \right. \end{array} \quad (6)$$

where P_s is the supply pressure of the pump, and P_r is the tank reference pressure. Similarly, let g_{3i} and g_{4i} be the square roots of the pressure drops for the ith hydraulic loop. For simplicity of notation, define the diagonal square root matrices of the pressure drops as:

$$\begin{array}{l} g_3(P_1, sign(x_v)) = diag[g_{31}(P_{11}, sign(x_{v1})), \ldots, g_{3n}(P_{1n}, sign(x_{vn}))] \\ g_4(P_2, sign(x_v)) = diag[g_{41}(P_{21}, sign(x_{v1})), \ldots, g_{4n}(P_{2n}, sign(x_{vn}))] \end{array} \quad (7)$$

Then, Q_1 and Q_2 in (5) are related to the spool displacements of the valves x_v by (Merritt, 1967),

$$Q_1 = k_{q1} g_3(P_1, sign(x_v)) x_v \ , Q_2 = k_{q2} g_4(P_2, sign(x_v)) x_v \quad (8)$$

where $k_{q1} = diag[k_{q11}, \ldots, k_{q1n}]$ and $k_{q2} = diag[k_{q21}, \ldots, k_{q2n}]$ are the *constant* flow gain coefficients matrices of the forward and return loops respectively.

Given the desired motion trajectory $q_d(t)$, the objective is to synthesize a control input $u = x_v$ such that the output $y = q$ tracks $q_d(t)$ as closely as possible in spite of various model uncertainties.

3 Adaptive Robust Controller Designs

3.1 Design Model and Issues to be Addressed

In this paper, for simplicity, we consider the parametric uncertainties due to the unknown payload m_L, and the nominal value of the lumped disturbance T, T_n only. Other parametric ucnertainties can be dealt with in the same way if necessary. In order to use parameter adaptation to reduce parametric uncertainties and improve performance, it is necessary to linearly parametrize the system dynamics equation in terms of a set of unknown parameters. To achieve this, define the unknown parameter set as $\theta = [\theta_1, \theta_2^T]^T$ where $\theta_1 = m_L$ and $\theta_2 = T_n$. The system dynamic equations can thus be linearly parametrized in terms of θ as

$$\begin{array}{l} M(q)\ddot{q} + C(q,\dot{q})\dot{q} + G(q) = \frac{\partial x}{\partial q}(A_1 P_1 - A_2 P_2) \\ \quad + \theta_2 + \tilde{T}(t,q,\dot{q}), \quad \tilde{T} = T(t,q,\dot{q}) - T_n \\ \dot{P}_1 = \beta_e V_1^{-1}(q)\left[-A_1\frac{\partial x}{\partial q}\dot{q} + Q_1(u, g_3(P_1, sign(u)))\right] \\ \dot{P}_2 = \beta_e V_2^{-1}(q)\left[A_2\frac{\partial x}{\partial q}\dot{q} - Q_2(u, g_4(P_2, sign(u)))\right] \end{array} \quad (9)$$

Since the extent of the parametric uncertainties and uncertain nonlinearities are normally known, the following practical assumption is made. Parametric uncertainties and uncertain nonlinearities satisfy

$$\begin{array}{l} \theta \in \Omega_\theta \stackrel{\Delta}{=} \{\theta : \ \theta_{min} < \theta < \theta_{max} \} \\ |\tilde{T}(t,q,\dot{q})| \leq \delta_T(q,\dot{q},t) \end{array} \quad (10)$$

where $\theta_{min} = [\theta_{1min}, \theta_{2min}]^T$, $\theta_{max} = [\theta_{1max}, \theta_{2max}]^T$, and $\delta_T(t,q,\dot{q})$ are known.

At this stage, it can be seen that the main difficulties in controlling (9) are: (i) The system dynamics are highly nonlinear and coupled, due to either the nonlinear robot dynamics or the dependence of the effective driving torque on joint angle (terms like $\frac{\partial x(q)}{\partial q}$) and the nonlinearities in the hydraulic dynamics; (ii) The system has large extent of parametric uncertainties due to the large variations of inertial load m_L; (iii) The system may have large extent of lumped uncertain nonlinearities $\tilde{T}$ including external disturbances and unmodeled friction forces; (iv) The added nonlinear hydraulic dynamics are more complex than the electrical motor dynamics; (v) The model uncertainties are mismatched, i.e. both parametric uncertainties and uncertain nonlinearities appear in the dynamic equations which are not directly related to the control input $u = x_v$.

To address the challenges mentioned above, following general strategies have been adopted in the controller designs in (Bu and Yao, 2000; Bu and Yao, 2001). Firstly, the nonlinear physical model based analysis and synthesis has been employed to deal with the nonlinearities and coupling of the system dynamics. Secondly, the ARC approach (Yao and Tomizuka, 1994; Yao, 1997) has been used to handle the effect of both parametric uncertainties and uncertain nonlinearities; fast robust feedback was used to attenuate the effect of various model uncertainties as much as possible while parameter adaptation was introduced to reduce model uncertainties for high performance. Thirdly, backstepping design via ARC Lyapunov function has been used to overcome the design difficulties caused by the unmatched model uncertainties. To avoid the need for joint acceleration by backstepping design, two methods have been presented in (Bu and

Yao, 2000; Bu and Yao, 2001) respectively, which are briefly reviewed in the following for later's comparative studies.

3.2 Controller Design

The design parallels the recursive backstepping design procedure via ARC Lyapunov functions in (Yao, 1997; Yao et al., 2000) as follows.

Step 1

The first step in both methods (Bu and Yao, 2000; Bu and Yao, 2001) is the same as follows. Define a switching-function-like quantity as $z_2 = \dot{z}_1 + k_1 z_1 = \dot{q} - \dot{q}_r$, where $\dot{q}_r = \dot{q}_d - k_1 z_1$, $z_1 = q - q_d(t)$, in which $q_d(t)$ is the reference trajectory and k_1 is a positive feedback gain. The design in this step is to make z_2 as small as possible with a guaranteed transient performance.

Define the load pressure as $P_L = A_1 P_1 - A_2 P_2$. If we treat P_L as the virtual control input, a virtual control law P_{Ld} for P_L can be synthesized such that z_2 is as small as possible with a guaranteed transient performance. The control function P_{Ld} consists of two parts given by

$$\begin{aligned} P_{Ld}(q,\dot{q},\hat{\theta}_1,\hat{\theta}_2,t) &= P_{Lda} + P_{Lds} \\ P_{Lda} &= (\tfrac{\partial x}{\partial q})^{-1}[\hat{M}\ddot{q}_r + \hat{C}(\dot{q},q)\dot{q}_r + \hat{G}(q) - \hat{\theta}_2 - K_2(t)z_2] \end{aligned} \tag{11}$$

where $K_2(t)$ is a positive feedback gain matrix and

$$\begin{aligned} &\hat{M}(q) = M_c + M_L\hat{\theta}_1 \quad \hat{C}(\dot{q},q) = C_c + C_L\hat{\theta}_1 \\ &\hat{G}(q) = G_c + G_L\hat{\theta}_1 \end{aligned} \tag{12}$$

P_{Lds} can be chosen to satisfy:

$$\begin{aligned} &\text{condition i} \qquad z_2^T[\tfrac{\partial x}{\partial q}P_{Lds} - \phi_2\tilde{\theta} + \tilde{T}] \le \varepsilon_2 \\ &\text{condition ii} \qquad z_2^T \tfrac{\partial x}{\partial q}P_{Lds} \le 0 \end{aligned} \tag{13}$$

where $\phi_2 = [-M_L\ddot{q}_r - C_L(\dot{q},q)\dot{q}_r - G_L(q), I_{n\times n}]$, and ε_2 is a design parameter which can be arbitrarily small. The adaptive function τ_2 is given by $\tau_2 = \phi_2 z_2$

Step 2

In this step, an actual control law is synthesized so that $z_3 = P_L - P_{Ld}$ converges to zero or a small value with a guaranteed transient performance and accuracy. If we were to use the backstepping design strategy via ARC Lyapunov function as in (Yao et al., 2000; Yao, 1997), the resulting ARC law would require the feedback of the joint acceleration $\ddot{q}$ since $\ddot{q}$ is needed in computing $\hat{P}_{Ld}$, the calculable part of the derivative of the desired virtual control function P_{Ld}, for adaptive model compensation. In order to avoid the need for joint acceleration feedback, two methods were presented in (Bu and Yao, 2000; Bu and Yao, 2001) respectively; one is observer based and the other is over-parametrization based as outlined in the following:

Observer based Design

Define the observer errors as:

$$\begin{aligned} &e_{o1} = q - y, \qquad \dot{y}_r = \dot{y} - k_{o1}e_{o1} \\ &e_{o2} = \dot{q} - \dot{y}_r, \qquad \ddot{y}_r = \ddot{y} - k_{o1}(\dot{q} - \dot{y}) \end{aligned} \tag{14}$$

where y and $\dot{y}$ are the estimates of q and $\dot{q}$ respectively. The following nonlinear observer was proposed :

$$\begin{aligned} \bar{M}(q)\ddot{y}_r + \bar{C}(q,\dot{q})\dot{y}_r + \bar{G}(q) &= \tfrac{\partial x}{\partial q}P_L \\ &+ (K_{o2} + K_{o2s})e_{o2} + T_{os} + \bar{\theta}_2 \end{aligned} \tag{15}$$

where $\bar{M}(q) = M_c + \underline{M}_L\bar{\theta}_{\underline{1}}$, $\bar{C}(q,\dot{q}) = C_c + C_L\bar{\theta}_1$ and $\bar{G}(q) = G_c + G_L\bar{\theta}_1$, in which $\bar{\theta} = [\theta_1, \theta_2]^T$ is a new set of parameter estimate for θ and is used in the construction of the above observer only. K_{o2} is any positive definite gain matrix, and K_{o2s} is a nonlinear positive definite gain matrix to be specified later. T_{os} is a robust observer error feedback term which is specified later for a guaranteed transient performance.

If the parameter variation $\tilde{\theta}_o = \theta - \bar{\theta}$ is within certain limit such that $\|\tilde{\theta}_{o\underline{1}}M_L q\bar{M}^{-1}(q)\| < 1$, then, a robust feedback function $T_{os}(q,\dot{q},\theta,y,\dot{y},t)$ can be determined to satisfy following conditions (Bu and Yao, 2000):

$$\begin{aligned} &\text{condition i} \quad e_{o2}^T[-(I - \tilde{\theta}_{o1}M_L\bar{M}^{-1})T_{os} + \phi_o^T\tilde{\theta}_o + \tilde{T}] \le \varepsilon_o \\ &\text{condition ii} \quad -e_{o2}^T(I - \tilde{\theta}_{o1}M_L\bar{M}^{-1})T_{os} \le 0 \end{aligned} \tag{16}$$

where $\phi_o = [M_L(q)\bar{M}^{-1}(\tfrac{\partial x}{\partial q}P_L + (K_{o2}+K_{o2s})e_{o2} + \bar{\theta}_2 - \bar{C}(q,\dot{q})\dot{y}_r - \bar{G}(q)) + C_L(q,\dot{q})\dot{y}_r + G_L(q), -I_{3\times 3}, 0]^T$ and ε_o is a positive design parameter. The adaptation law for parameter estimates in observer is given by

$$\dot{\bar{\theta}} = Proj_{\bar{\theta}}(\Gamma_o\tau_o), \qquad \tau_o = \phi_o^T e_{o2} \tag{17}$$

From (15), $\ddot{y}_r$ can be computed by:

$$\begin{aligned} \ddot{y}_r = \bar{M}^{-1}(q)[&\tfrac{\partial x}{\partial q}P_L + (K_{o2} + K_{o2s})e_{o2} + T_{os} \\ &+ \bar{\theta}_2 - \bar{C}(q,\dot{q})\dot{y}_r - \bar{G}(q)] \end{aligned} \tag{18}$$

and can be used in the design of the control law u.

Note that $\dot{y}_r$ and $\ddot{y}_r$ are the estimates of the joint velocity and acceleration respectively. By using the velocity estimate $\dot{y}_r$ to replace the joint velocity $\dot{q}$ in the virtual control law P_{Ld}, we obtain the estimate of the P_{Ld} as $\hat{P}_{Ld} = P_{Ld}(q,\dot{y}_r,\hat{\theta}_1,\hat{\theta}_2,t)$.

The following is to synthesize a control input u such that $\hat{z}_3 = P_L - \hat{P}_{Ld}$ converges to zero or a small value with a guaranteed transient performance. From (9),

$$\begin{aligned} \dot{\hat{z}}_3 = \dot{P}_L - \dot{\hat{P}}_{Ld} = \theta_3[&-(A_1^2V_1^{-1} + A_2^2V_2^{-1})\tfrac{\partial x}{\partial q}\dot{q} \\ &+ (A_1V_1^{-1}Q_1 + A_2V_2^{-1}Q_2)] - \dot{\hat{P}}_{Ld} \end{aligned} \tag{19}$$

where $\dot{\hat{P}}_{Ld} = \tfrac{\partial \hat{P}_{Ld}}{\partial q}\dot{q} + \tfrac{\partial \hat{P}_{Ld}}{\partial \dot{y}_r}\ddot{y}_r + \tfrac{\partial \hat{P}_{Ld}}{\partial t} + \tfrac{\partial \hat{P}_{Ld}}{\partial \theta}\dot{\hat{\theta}}$. Define the load flow Q_L as

$$\begin{aligned} Q_L = A_1V_1^{-1}Q_1 + A_2V_2^{-1}Q_2 = [&A_1V_1^{-1}k_{q1}g_3(P_1, sign(u)) \\ &+ A_2V_2^{-1}k_{q2}g_4(P_2, sign(u))]u \end{aligned} \tag{20}$$

then this step is to synthesize a control function Q_{Ld} for Q_L such that P_L tracks the desired control function $\hat{P}_{Ld}$ with a guaranteed transient performance. The control function Q_{Ld} consists of two parts given by

$$\begin{aligned} &Q_{Ld}(q,\dot{q},\dot{y}_r,\ddot{y}_r,P_1,P_2,\hat{\theta},t) = Q_{Lda} + Q_{Lds} \\ &Q_{Lda} = -\tfrac{1}{\hat{\theta}_3} Q_{Lde} \\ &Q_{Lds} = Q_{Lds1} + Q_{Lds2},\ \ Q_{Lds1} = -\tfrac{1}{\theta_{3min}} K_3 \hat{z}_3 \end{aligned} \tag{21}$$

where K_3 is a constant positive definite control gain matrix, $Q_{Lde} = \frac{\partial x}{\partial q} z_2 - \hat{\theta}_3 (A_1^2 V_1^{-1} + A_2^2 V_2^{-1}) \frac{\partial x}{\partial q} \dot{q} - \dot{\hat{P}}_{Ld}$, and Q_{Lds2} is a robust control function satisfying the following two conditions

$$\begin{aligned} &\text{condition i} \qquad \hat{z}_3^T \left[\theta_3 Q_{Lds2} + \phi_3^T \tilde{\theta}\right] \le \varepsilon_3 \\ &\text{condition ii} \qquad \hat{z}_3^T Q_{Lds2} \le 0 \end{aligned} \tag{22}$$

where $\phi_3 = [0, 0, -Q_{La} + (A_1^2 V_1^{-1} + A_2^2 V_2^{-1}) \frac{\partial x}{\partial q} \dot{q}]^T$ and ε_3 is a positive design parameter.

Once the control function Q_{Ld} for Q_L is synthesized as given by (21), the actual control input u can be backed out from the continuous one-to-one nonlinear load flow mapping (20) as follows. Noting that the elements of the diagonal matrices g_3, g_4, V_1, and V_2 are all positive functions, u_i should have the same sign as Q_{Ldi}. Thus

$$\begin{aligned} u = [&A_1 V_1^{-1} k_{q1} g_3(P_1, sign(Q_{Ld})) \\ &+ A_2 V_2^{-1} k_{q2} g_4(P_2, sign(Q_{Ld}))]^{-1} Q_{Ld} \end{aligned} \tag{23}$$

The parameter estimation law is given by

$$\dot{\hat{\theta}} = Proj_{\hat{\theta}}(\Gamma(\tau_2 + \phi_3 \hat{z}_3)) \tag{24}$$

where the projection mapping used here is defined as in (Sastry and Bodson, 1989; Goodwin and Mayne, 1989; Yao and Tomizuka, 1994) and Γ is the diagonal adaptation gain matrix.

Overparametrizing Design

In the above, an observer based method is presented to avoid the need for joint acceleration feedback. In the following, a different method proposed in (Bu and Yao, 2001) is shown, which utilizes the linearly parametrization property of the inertia matrix in (4).

Multiply both side of first equation of (9) by $|M|M^{-1} = \bar{M}$ we will have

$$|M|\ddot{q} + \bar{M}C(\dot{q},q)\dot{q} + \bar{M}G = \bar{M}\tfrac{\partial x}{\partial q} P_L + \bar{M}\theta_2 + \bar{M}\tilde{T} \tag{25}$$

Define

$$\begin{aligned} &C_t(\dot{q},q) = \bar{M}C(\dot{q},q) \quad G_t(q) = \bar{M}G \\ &d_n = \bar{M}\theta_2 \quad \tilde{d} = \bar{M}\tilde{T} \end{aligned} \tag{26}$$

Thus (25) could be expressed by

$$I\ddot{q} + C_t\dot{q} + G_t = \bar{M}\tfrac{\partial x}{\partial q} P_L + d_n + \tilde{d} \tag{27}$$

where I is a scalar. Similar to (2), C_t, G_t and d_n can be expressed by

$$\begin{aligned} &C_t(\dot{q},q) = C_{tc} + \textstyle\sum_{i=1}^n C_{ti}\theta_1^i \quad G_t(q) = G_{tc} + \sum_{i=1}^n G_{ti}\theta_1^i \\ &d_n = \bar{M}_c\theta_2 + \textstyle\sum_{i=1}^{n-1} \bar{M}_i\theta_1^i\theta_2 \end{aligned} \tag{28}$$

where C_{tc} and G_{tc} are of the known nonlinear functions of q and $\dot{q}$.

From (28), redefine the unknown parameters as:

$$\begin{aligned} &[\beta_1, \beta_2, \cdots, \beta_n, \beta_{n+1}^T, \beta_{n+2}^T, \cdots, \beta_{2n}^T] \\ &= [\theta_1, \theta_1^2, \cdots, \theta_1^n, \theta_2^T, \theta_1\theta_2^T, \cdots, \theta_1^{n-1}\theta_2^T] \end{aligned} \tag{29}$$

From (9), the derivative of z_3 is given by

$$\begin{aligned} &\dot{z}_3 = \dot{P}_L - \dot{P}_{Ld} \\ &\dot{P}_L = \beta_e[-(A_1^2 V_1^{-1} + A_2^2 V_2^{-1})\tfrac{\partial x}{\partial q}\dot{q} + (A_1 V_1^{-1} Q_1 + A_2 V_2^{-1} Q_2)] \\ &\dot{P}_{Ld} = \tfrac{\partial P_{Ld}}{\partial q}\dot{q} + \tfrac{\partial P_{Ld}}{\partial \dot{q}}\ddot{q} + \tfrac{\partial P_{Ld}}{\partial \hat{\theta}}\dot{\hat{\theta}} + \tfrac{\partial P_{Ld}}{\partial t} \end{aligned} \tag{30}$$

and $I\dot{P}_{Ld}$ can be expressed by

$$I\dot{P}_{Ld} = \widehat{I\dot{P}_{Ld}} + \widetilde{I\dot{P}_{Ld}} \tag{31}$$

where

$$\begin{aligned} &\widehat{I\dot{P}_{Ld}} = \tfrac{\partial P_{Ld}}{\partial q}\hat{I}\dot{q} + \tfrac{\partial P_{Ld}}{\partial \dot{q}}(-\hat{C}_t\dot{q} - \hat{G}_t + \hat{\bar{M}}\tfrac{\partial x}{\partial q}P_L + \hat{d}_n) \\ &\qquad + \tfrac{\partial P_{Ld}}{\partial \hat{\theta}}\hat{I}\dot{\hat{\theta}} + \tfrac{\partial P_{Ld}}{\partial t}\hat{I} \\ &\widetilde{I\dot{P}_{Ld}} = (\tfrac{\partial P_{Ld}}{\partial q}\dot{q} + \tfrac{\partial P_{Ld}}{\partial \hat{\theta}}\dot{\hat{\theta}} + \tfrac{\partial P_{Ld}}{\partial t})(-\textstyle\sum_{i=1}^n I_{si}\tilde{\beta}_i) \\ &\qquad + \tfrac{\partial P_{Ld}}{\partial \dot{q}}[\textstyle\sum_{i=1}^n (C_{ti}\dot{q} + G_{ti})\tilde{\beta}_i - \sum_{i=1}^{n-1}\bar{M}_i\tfrac{\partial x}{\partial q}P_L\tilde{\beta}_i - \bar{M}_c\tilde{\beta}_{n+1} \\ &\qquad - \textstyle\sum_{i=2}^n \bar{M}_{i-1}\tilde{\beta}_{n+i} + \tilde{d}] \\ &\hat{I} = I_c + \textstyle\sum_{i=1}^n I_{si}\hat{\beta}_i, \quad \hat{C}_t = C_{tc} + \sum_{i=1}^n C_{ti}\hat{\beta}_i \\ &\hat{G}_t = G_{tc} + \textstyle\sum_{i=1}^n G_{ti}\hat{\beta}_i, \quad \hat{d}_n = \bar{M}_c\hat{\beta}_{n+1} + \sum_{i=2}^n \bar{M}_{i-1}\hat{\beta}_{n+i} \\ &\hat{\bar{M}} = \bar{M}_c + \textstyle\sum_{i=1}^{n-1}\bar{M}_i\hat{\beta}_i \end{aligned} \tag{32}$$

$\widehat{I\dot{P}_{Ld}}$ represents the calculable part of $I\dot{P}_{Ld}$ and will be used in the model compensation part of the ARC control law in this step, $\widetilde{I\dot{P}_{Ld}}$ is the incalculable part of $I\dot{P}_{Ld}$ and will be attenuated by certain robust feedback. Similar to the observer based design, the control function Q_{Ld} is given by

$$\begin{aligned} &Q_{Ld} = Q_{Lda} + Q_{Lds} \\ &\quad Q_{Lda} = (A_1^2 V_1^{-1} + A_2^2 V_2^{-1})\tfrac{\partial x}{\partial q}\dot{q} \\ &\qquad + \tfrac{1}{\hat{I}\beta_e}(-\tfrac{\partial x}{\partial q}z_2 + \widehat{I\dot{P}_{Ld}} - \tfrac{1}{2}\hat{\dot{I}}z_3 - I_c K_3 z_3) \end{aligned} \tag{33}$$

where $\hat{I} = \dot{I}_c + \sum_{i=1}^{n} \dot{I}_{si}\hat{\beta}_i$ and K_3 is a positive feedback gain matrix. Q_{Lds} could be chosen to satisfy:

$$\begin{array}{ll} \text{condition i} & z_3^T(I\beta_e Q_{Lds} - \phi_3\tilde{\beta} - \frac{\partial P_{Ld}}{\partial \dot{q}}\tilde{d}) \le \varepsilon_3 \\ \text{condition ii} & z_3^T I\beta_e Q_{Lds} \le 0 \end{array} \tag{34}$$

where ε_3 is a positive design parameter and $\phi_3 = [\phi_{3(1)}, \cdots, \phi_{3(n-1)}, \phi_{3n}, \phi_{3(n+1)}, \phi_{3(n+2)}, \cdots, \phi_{3(2n)}]$.

$$\begin{aligned} \phi_{3(1)} &= I_{s1}[\beta_e Q_{Lda} - \beta_e(A_1^2V_1^{-1} + A_2^2V_2^{-1})\tfrac{\partial x}{\partial q}\dot{q} - \tfrac{\partial P_{Ld}}{\partial q}\dot{q} \\ &\quad - \tfrac{\partial P_{Ld}}{\partial \theta}\dot{\hat{\theta}} - \tfrac{\partial P_{Ld}}{\partial t}] + \tfrac{\partial P_{Ld}}{\partial \dot{q}}(C_{t1}\dot{q} + G_{t1} - \bar{M}_1\tfrac{\partial x}{\partial q}P_L) + \tfrac{1}{2}\dot{I}_{s1}z_3 \\ \phi_{3(n-1)} &= I_{sn-1}[\beta_e Q_{Lda} - \beta_e(A_1^2V_1^{-1} + A_2^2V_2^{-1})\tfrac{\partial x}{\partial q}\dot{q} \\ &\quad - \tfrac{\partial P_{Ld}}{\partial q}\dot{q} - \tfrac{\partial P_{Ld}}{\partial \theta}\dot{\hat{\theta}} - \tfrac{\partial P_{Ld}}{\partial t}] + \tfrac{\partial P_{Ld}}{\partial \dot{q}}(C_{tn-1}\dot{q} + G_{tn-1} \\ &\quad - M_{n-1}\tfrac{\partial x}{\partial q}P_L) + \tfrac{1}{2}\dot{I}_{sn-1}z_3 \\ \phi_{3n} &= I_{sn}[\beta_e Q_{Lda} - \beta_e(A_1^2V_1^{-1} + A_2^2V_2^{-1})\tfrac{\partial x}{\partial q}\dot{q} \\ &\quad - \tfrac{\partial P_{Ld}}{\partial q}\dot{q} - \tfrac{\partial P_{Ld}}{\partial \theta}\dot{\hat{\theta}} - \tfrac{\partial P_{Ld}}{\partial t}] + \tfrac{\partial P_{Ld}}{\partial \dot{q}}(C_{tn}\dot{q} + G_{tn}) + \tfrac{1}{2}\dot{I}_{sn}z_3 \\ \phi_{3(n+1)} &= -\tfrac{\partial P_{Ld}}{\partial \dot{q}}\bar{M}_c \quad \phi_{3(n+2)} = -\tfrac{\partial P_{Ld}}{\partial \dot{q}}\bar{M}_1 \quad \phi_{3(2n)} = -\tfrac{\partial P_{Ld}}{\partial \dot{q}}\bar{M}_{n-1} \end{aligned} \tag{35}$$

The control input u can then be back out as shown in (23).

The parameter estimates in the overparametrizing method are updated by

$$\begin{aligned} \dot{\hat{\theta}} &= Proj_{\hat{\theta}}(\Gamma_\theta \tau_2) \\ \dot{\hat{\beta}} &= Proj_{\hat{\beta}}(\Gamma_\beta \phi_3 z_3) \end{aligned} \tag{36}$$

where Γ_θ and Γ_β are diagonal adaptation gain matrices.

4 Comparative Simulation Results

To study fundamental problems associated with the control of electro-hydraulic systems, a three-link robot arm driven by three single-rod hydraulic cylinders shown in Fig.1 has been set up. The detailed experimental set up can be found in (Yao et al., 2000). Although some preliminary experimental results have been obtained in (Bu and Yao, 2000; Bu and Yao, 2001) for the proposed two methods respectively, to better illustrate the advantages and the disadvantages of the two methods, comparative simulations instead of experiments are conducted in the following as simulations allow us to consider various scenarios instead of being limited by the current physical hardware used. For example, the valve bandwidth of current experimental system is quite low and has a significant effect on the achievable control performance. Only simulation allows us to compare the performance robustness of the two methods to other practical factors such as the measurement noises without considering the effect of low bandwidth valves.

The simulations are run based on the physical model of the hydraulic arm shown in Fig.1 except neglecting the valve dynamics as assumed in the paper. The exact model of the hydraulic arm is quite messy and can be obtained from the authors. Parameters of the actual arm used in the simulations are: m_1 =22.98kg, m_2 =24.94kg, m_3 =19.68kg, l_1 =0.3683m, l_2= 0.9906m, and l_3 =0.8001m. Hydraulic cylinder parameters are: $A_1 = diag[2.0268\times10^{-3}, 2.0268\times10^{-3}, 2.0268\times10^{-3}]m^2$, $A_2 = diag[1.0688\times10^{-3}, 1.0688\times10^{-3}, 1.0688\times10^{-3}]m^2$, $V_{h1} = diag[4.9953\times10^{-4}, 5.2125\times10^{-4}, 4.8505\times10^{-4}]m^3$, and $V_{h2} = diag[9.0676\times10^{-4}, 8.7237\times10^{-4}, 9.2667\times10^{-4}]m^3$. The valve parameters are $k_{q1} = diag[3.5904\times10^{-8}, 3.5904\times10^{-8}, 3.5904\times10^{-8}]\frac{m^3}{sec\sqrt{Pa}V}$ and $k_{q2} = diag[3.7206\times10^{-8}, 3.7206\times10^{-8}, 3.7206\times10^{-8}]\frac{m^3}{sec\sqrt{Pa}V}$. The supplied pressure is $P_s = 6.9\times10^6 Pa$ and actual bulk modulus is $\beta_e = 2.7148\times10^8 Pa$.

The following three controllers are compared:

Independent ARC Controller .

The ARC controllers proposed in (Bu and Yao, 1999; Yao et al., 2000) are applied to individual joints of the robot without considering the coupling among various joints.

Observer based ARC Controller .

The control gain and gain matrices are chosen as $k_1 = 200$, $K_2 = K_3 = diag[310, 250, 240]$, $k_{o1} = 500$, and $K_{o2} = diag[500, 1000, 1000]$. Adaptation gain matrices are $\Gamma = diag[1, 100, 120, 140]$ and $\Gamma_o = diag[100, 200, 300, 400]$.

Overparametrizing ARC Method .

The control gain and gain matrices are chosen as $k_1 = 160$, $K_2 = diag[160, 200, 220]$, $K_3 = diag[160, 200, 220]$. Adaptation gain matrices are $\Gamma_\theta = diag[35,\ 1\times10^{-6},\ 1\times10^{-6},\ 1\times10^{-6}]$ and $\Gamma_\beta = diag[30, 2\times10^{-9},\ 2\times10^{-7}, 1\times10^{-8},\ 1\times10^{-7},\ 1\times10^{-7}, 1\times10^{-9},\ 1\times10^{-8},\ 1\times10^{-8}, 1\times10^{-10},\ 1\times10^{-9},\ 1\times10^{-9}]$.

The desired trajectories for the simulation are chosen to be typical point-to-point motion as shown in Fig.2. The maximum velocity of the trajectory is $v_{max} = 0.6 rad/s$ and the maximum acceleration is $a_{max} = 6 rad/s^2$. The simulations are running for the following scenarios.

Case 1: no load .

In this case, there is no load installed at the end of robot arm. The tracking results are shown in Fig.3, Fig.4 and Fig.5. As shown in the figures, compared with the independent ARC controller, both the coordinated ARC controllers t achieve an order of tracking error reduction, which demonstrates the need for explicitly considering the coupling effect among various joints. It is also seen that the overparametrizing ARC method achieves a better tracking performance than the observer based ARC method. Fig.6 shows the control input for the swing valve, which is regular. The control inputs for the other two valves show similar behavior and are omitted.

Case 2: with load .

In this case, a 30kg external load is added at the end of robot arm (e.g. $m_L = \theta_1 = 30$) to test the performance robustness of the two coordinated ARC algorithms to load variations. The tracking errors are shown in Fig.7, Fig.8, and Fig.9 respectively. As seen from the figures, both methods have the same level of tracking errors as in no-load situations, which verifies the performance robustness of the proposed ARC methods. Again, the overparametrizing method

achieves a slightly better tracking performance. The control inputs for the swing joint are shown in Fig.10, which is regular. The parameter estimations for the external load (not shown) reveal that the load estimate in the observer based ARC method converges to its true value while the overparametrizing ARC method does not, due to the large number of parameters adapted in the overparametrizing method.

Case 3: with sensor noise .

To further illustrate the advantages and disadvantages of both methods, the sensor noises are added in this case. The tracking results are shown in Fig.11, Fig.12 and Fig.13. As seen from the swing control inputs shown in Fig.14, the observer based ARC method is more sensitive to the sensor noise, which results in a poorer tracking performance.

5 Conclusion

In this paper, some comparative studies were carried out for the two recently proposed coordinated ARC controllers for robotic manipulators driven by single-rod hydraulic actuators. The first ARC method relies on an ARC observer to recover the state needed for the ARC backstepping design. The second method utilizes the property that the adjoint matrix and the determinant of the inertial matrix could be linearly parametrized by certain suitably selected parameters and employs overparametrizing techniques. Although the same theoretical performance can be achieved by both ARC methods, comparative simulation results show that, in general, the overparametrization method achieves a little better tracking performance, although parameter estimates may not converge as well as those in the observer based method. The biggest advantage of the overparametrization method is its ability of being less noise sensitive. Such an advantage will become apparent in implementation as electro-hydraulic systems normally have quite significant amount of measurement noises.

REFERENCES

Bridges, M. M., Dawson, D. M., and Abdallah, C. T. (1993). Control of rigid-link flexible-joint robots: a survey of backstepping approaches. In *ASME winter annual meeting, DSC-Vol 49*, pages 177–189.

Bu, F. and Yao, B. (1999). Adaptive robust precision motion control of single-rod hydraulic actuators with time-varying unknown inertia : a case study. In *ASME International Mechanical Engineering Congress and Exposition (IMECE), FPST-Vol.6,*, pages 131–138, Nashville, TN.

Bu, F. and Yao, B. (2000). Observer based coordinated adaptive robust control of robot manipulators driven by single-rod hydraulic actuators. In *Proc. of IEEE International Conference on Robotics and Automation*, pages 3034–3039, San Francisco.

Bu, F. and Yao, B. (2001). Nonlinear model based coordinated adaptive robust control of electro-hydraulic robotic manipulator by overparametrizing method. In *Proc. of IEEE International Conf. on Robotics and Automation (ICRA)*, pages 3459–3464, Seoul, Korean.

d'ANdrea Novel, B., M.A.Garnero, and Abichou, A. (1994). Nonlinear control of a hydraulic robot using singular perturbations. In *Proc. of IEEE Conf. on Robotics and Automation*, pages 1932–1937.

Goodwin, G. C. and Mayne, D. Q. (1989). A parameter estimation perspective of continuous time model reference adaptive control. *Automatica*, 23(1):57–70.

Medanic, J., Yuan, M., and Medanic, B. (1997). Robust multivariable nonlinear control of a two link excavator: Part i. In *Proceedings of the 36th Conference on Decision and Control*, pages 4231–4236.

Merritt, H. E. (1967). *Hydraulic control systems*. Wiley, New York.

Sastry, S. and Bodson, M. (1989). *Adaptive Control: Stability, Convergence and Robustness*. Prentice Hall, Inc., Englewood Cliffs, NJ 07632, USA.

Yao, B. (1997). High performance adaptive robust control of nonlinear systems: a general framework and new schemes. In *Proc. of IEEE Conference on Decision and Control*, pages 2489–2494, San Diego.

Yao, B., Bu, F., Reedy, J., and Chiu, G. (2000). Adaptive robust control of single-rod hydraulic actuators: theory and experiments. *IEEE/ASME Trans. on Mechatronics*, 5(1):79–91.

Yao, B. and Tomizuka, M. (1994). Smooth robust adaptive sliding mode control of robot manipulators with guaranteed transient performance. In *Proc. of American Control Conference*, pages 1176–1180, Baltimore. The full paper appeared in *ASME Journal of Dynamic Systems, Measurement and Control*, Vol. 118, No.4, pp764-775, 1996.

Yao, B. and Tomizuka, M. (1997). Adaptive robust control of SISO nonlinear systems in a semi-strict feedback form. *Automatica*, 33(5):893–900. (Part of the paper appeared in Proc. of 1995 American Control Conference, pp2500-2505, Seattle).

Yao, B. and Tomizuka, M. (2001). Adaptive robust control of MIMO nonlinear systems in semi-strict feedback forms. *Automatica*, 37(9):1305–1321. Parts of the paper were presented in the *IEEE Conf. on Decision and Control*, pp2346-2351, 1995, and the *IFAC World Congress*, Vol. F, pp335-340, 1996.

Yuan, J. (1995). Adaptive control of robotic manipulators including motor dynamics. *IEEE Trans. on Robotics and Automation*, 11(4):612–617.

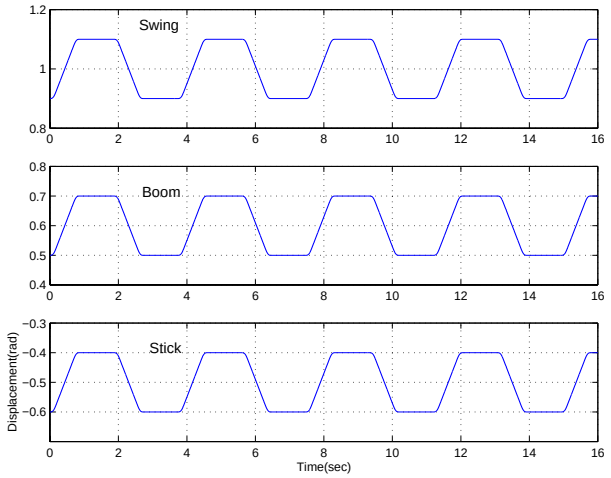

Figure 2. Desired trajectories for 3 joints

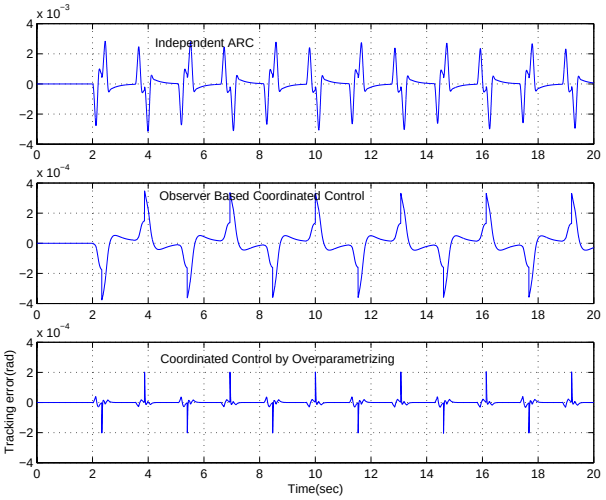

Figure 3. Tracking error for swing joint without load

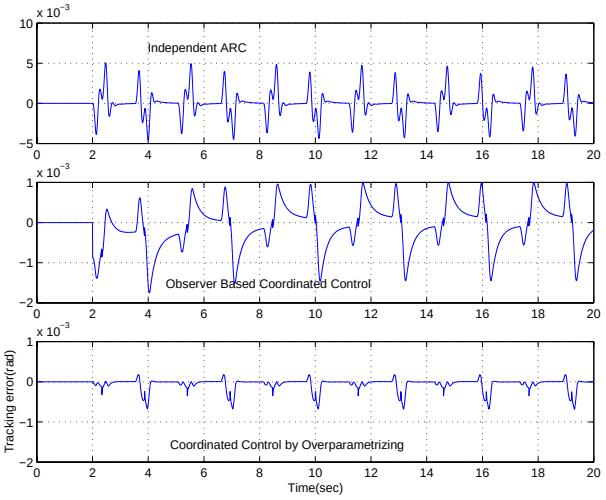

Figure 4. Tracking error for boom joint without load

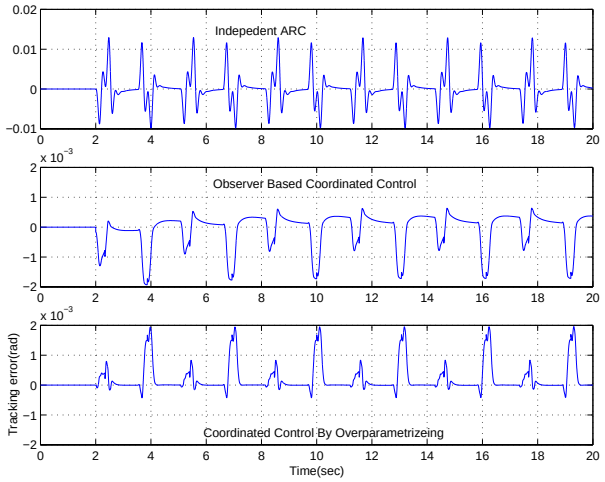

Figure 5. Tracking error for stick joint without load

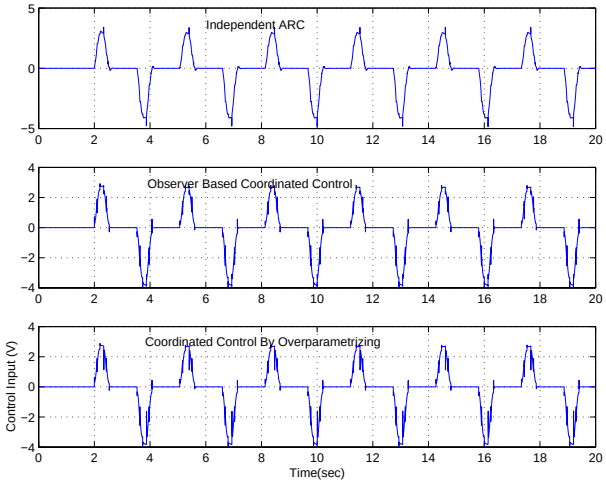

Figure 6. Control input for swing joint without load

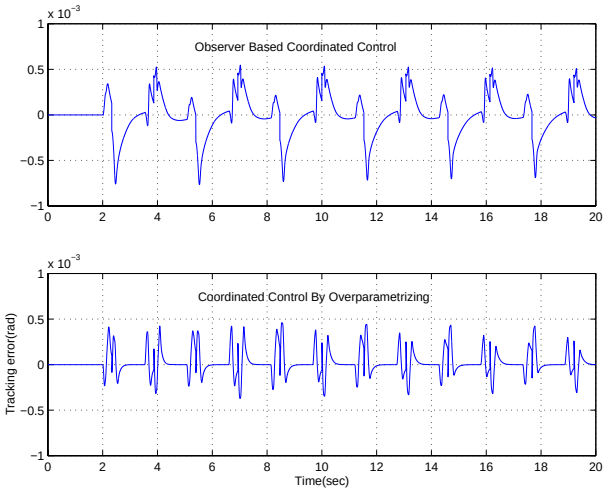

Figure 7. Tracking error for swing joint with load

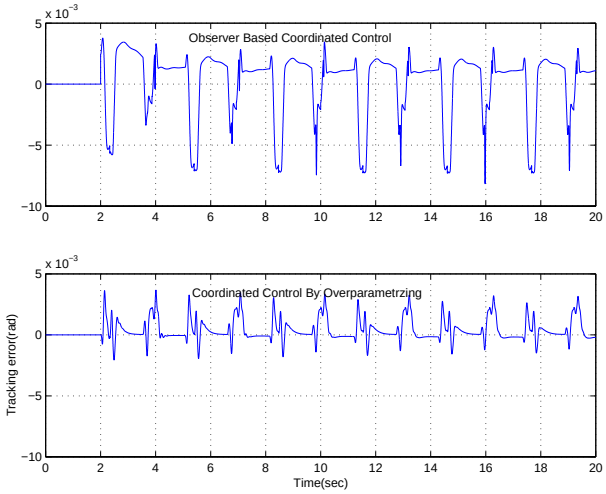

Figure 8. Tracking error for boom joint with load

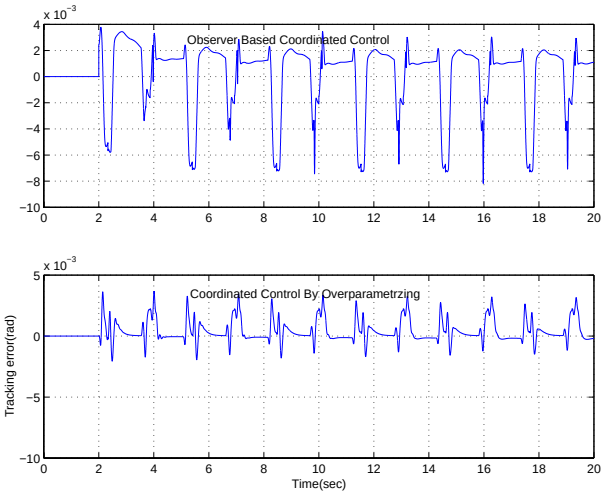

Figure 9. Tracking error for stick joint with load

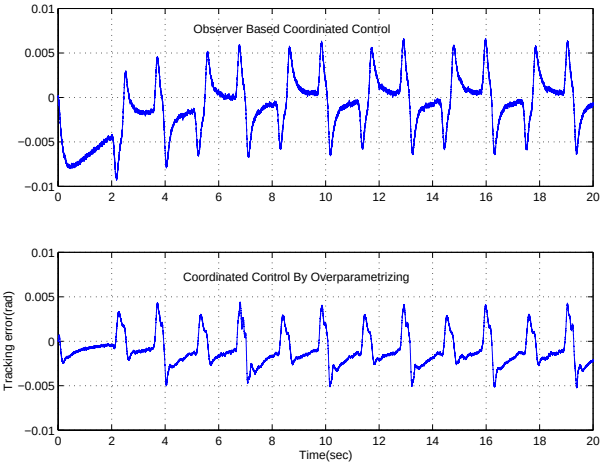

Figure 12. Tracking error for boom joint with noise

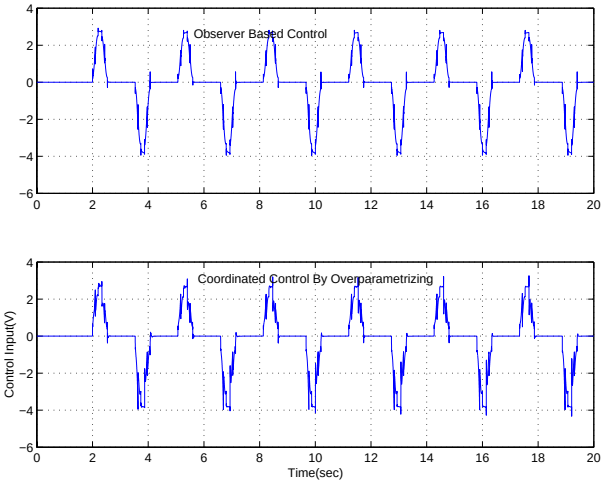

Figure 10. Control input for swing joint with load

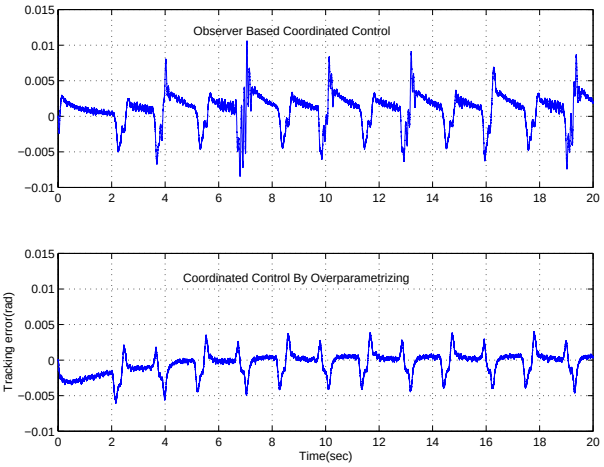

Figure 13. Tracking error for stick joint with noise

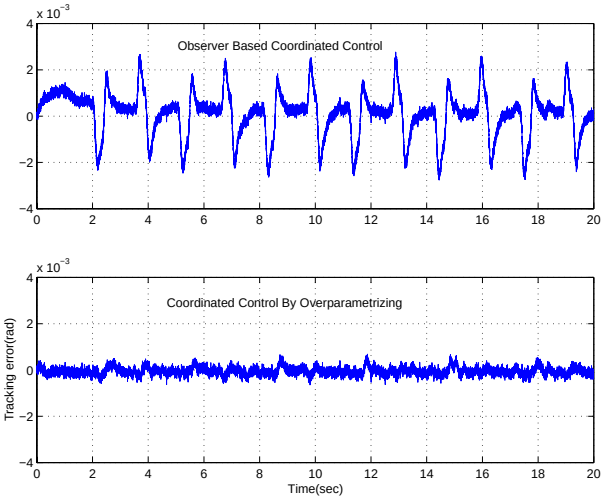

Figure 11. Tracking error for swing joint with noise

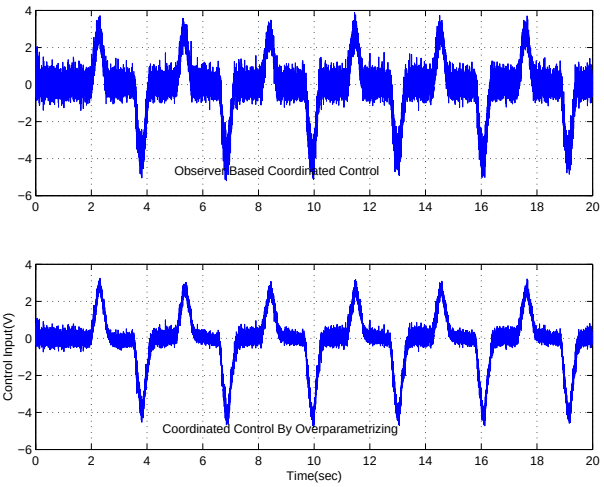

Figure 14. Control input for swing joint with noise